ANALYSIS OF THE INCOMING FLOW IN A BLOOD FILTER

Rudolf Huebner
Pontifícia Universidade Católica de Minas Gerais – Instituto Politécnico
Av. Dom José Gaspar, 500 – Coração Eucarístico – BH – MG - CEP 30535-610
rudolf@pucminas.br

Paolo Castellini
Università degli Studi di Ancona
Via Brecce Bianche, 60131 – Ancona – Italia
cast@mehp1.unian.it

Marcos Pinotti Barbosa
Universidade Federal de Minas Gerais – Departamento de Engenharia Mecânica
Av. Antônio Carlos, 6627 – Pampulha – BH – MG - CEP 31270-901
pinotti@demec.ufmg.br

Abstract. *Heart surgeries using extracorporeal circulation are a common practice. Artificial circulatory devices represent an indispensable tool in clinical practice. Blood flow through artificial devices is associated to red blood cells damage and/or thrombus formation. Is generally accepted that the presence of high turbulent shear stresses generated in the flow fields of artificial devices are partially responsible for the levels of red blood cells destruction, or hemolysis. Investigating the effect of turbulent shear stress on hemolysis is of prime importance to research work related to artificial devices. Hemolysis potential can be expressed as function of the shear stresses magnitude acting on blood cells and their exposure time to the shear stresses. The present work presents the use of two techniques used to study the incoming flow in an arterial blood filter. The general structure of the flow field was analyzed using the dye injection technique. A laser Doppler anemometer was used to measure two orthogonal velocity components and their fluctuations, which were used to determine the turbulent shear stresses. The exposure time was calculated and used in conjunction with the turbulent shear stresses to estimate the hemoglobin released by the red blood cells.*

Keywords. *Blood filter, LDA, Visualization, Hemolysis, Turbulence*

1. Introduction

Heart surgeries using extracorporeal circulation are a common practice. Artificial circulatory devices represent an indispensable tool in clinical practice. In an extracorporeal circulation circuit the blood is pumped using a pump, a device named oxygenator is used as gas and heat exchanger and some filters are installed at some points in the circuit and are used to filter the blood. The last filter is denominated arterial blood filter because it is placed in the arterial line of the circuit and is responsible to remove any particle present in the blood flow before the blood is returned to the patient. The arterial filter is used with the finality to minimize the occurrence of microembolization. Microembolization during an extracorporeal circulation is due to the presence of air bubbles, platelet aggregates and pieces of plastic. Microemboli can cause organ disfunction, mainly in the brain and lung.

Blood flow through artificial devices is associated with thrombus formation and/or red blood cell damage also called hemolysis. The presence of local vortices, secondary flows and low shear rates values may cause the formation of thrombi, platelet adhesion and aggregation as cited by Grigione et al. (2002). High values of shear stress are responsible for red blood cells and platelet destruction as shown by many works in the literature.

Sutera and Mehrjardi (1975) have shown that hemolysis can be induced at moderate shear stresses in the presence of a foreign surface. Prolonged exposure to turbulent shear stresses as low as 150 N/m² can produce lysis of red blood cells as shown by Sutera (1977). Experiments have demonstrated that the critical level of shear stress tolerable by a cell is highly dependent upon the exposure time. Sallam and Hwang (1984) have shown that incipient hemolysis begins at Reynolds stresses of about 400 N/m² for 1 ms of exposure. Paul et al. (1999) suggest that the resistance of red blood cells to shearing forces is higher, reaching a threshold of 500 N/m² for 1 ms of exposure. Lu et al. (2001) revised the threshold value to 800 N/m² with an exposure time of 1 ms.

Rand (1964) suggests an equation that correlates shear stress and exposure time. The equation has the form of $\tau^2.t$ = constant, where τ is the shear stress and t is the exposure time. This equation is comparable to the equation proposed by Wurzinger et al. (1985) which is an empirical correlation based on experimental data using a Couette viscometer. In this equation the percentage of released hemoglobin is given by

$$\frac{\Delta Hb}{Hb}\% = 3{,}62x10^{-5} t^{0{,}785} \tau_{\max}^{2{,}416} \tag{1}$$

where t is the exposure time (s) and τ_{max} is the maximum turbulent shear stress (N/m²). The equation above was used in this work to evaluate the percentage of released hemoglobin.

The aim of this work is to study the incoming flow in an arterial blood filter. The flow in some regions of the filter was studied using the laser Doppler velocimetry technique. For each region velocity and their fluctuations are

presented. Maximum turbulent stresses and exposure time were evaluated and used to estimate the percentage of released hemoglobin which can be regarded as a hemolytic potential.

2. Materials and Methods

2.1. The blood filter

The filter studied is used in cardiopulmonary bypass procedures. The body filter is made using acrylic and a polyester screen is used in the filtering element, which has a porosity of 40 μm. The filter inlet and outlet connectors have a diameter of 9,5 mm and are made of reinforced acrylic. The filter has a priming volume of about 280 ml, is projected to be used in adult patients and can be operated with a maximum flow rate of 6 liters per minute. The filter has a bypass line that can be used in situations where the filtering element pores are obstructed and another line is used to eliminate air trapped by the filter. Figure 1 shows a schematic view of the filter, its elements and the flow inside it. In figure 1, blue arrows are used to indicate unfiltered blood while red arrows indicate filtered blood

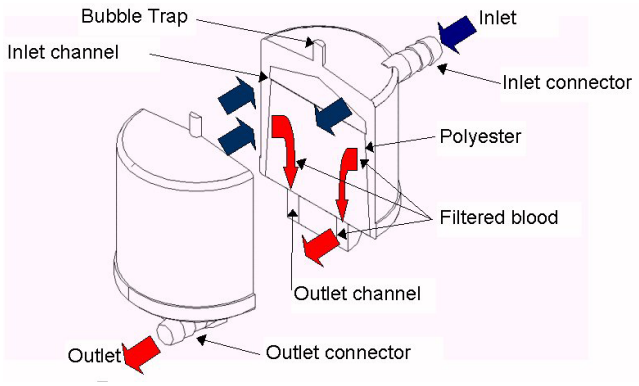

Figure 1. Schematic view of the filter and its elements

Blood flows through the inlet connector, located at the upper part of the filter, and describes a descending helical movement while it flows along the inlet channel. During this helical movement the blood flows through the filtering element, polyester, reaches the outlet channel and flows in direction of the outlet connector, located at the bottom of the filter.

2.2. The flow circuit

A test bench was assembled in order to reproduce the flow condition observed during a cardiopulmonary bypass. Figure 2 depicts schematically the test circuit.

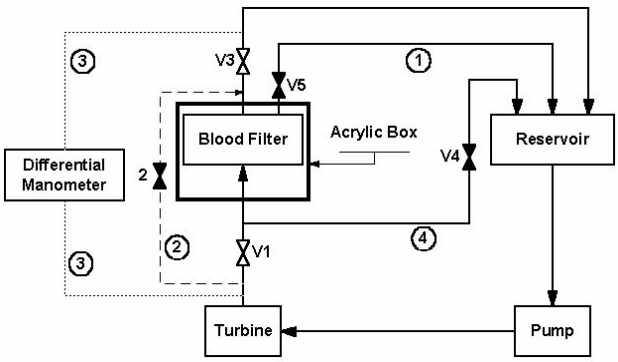

Figure 2 – Schematic view of the test circuit

Working fluid was pumped through the turbine and blood filter returning to the circuit reservoir. Line 1 represents the bubble trap and was used during the circuit filling up. During the LDA measurements many particles, necessary due to the LDA working principle, were captured by the filtering element and Lines 2 and 4 were used together to clean the filter using a retrograde flow. Pressure drop across the filter was monitored by a differential manometer, indicated by lines 3. Flow rate was monitored by a turbine flow meter and the pump rotating speed was controlled changing the excitation voltage of a brushless motor. All elements were connected using PVC flexible tubes. A prismatic acrylic box was used as optical window to minimize optical distortions. During the LDA measurements and flow visualization tests the filter was placed inside this prismatic box filled with water. The flow rate used in the LDA tests was 4.5 liters per

minute which is an accordance with the values used during a cardiopulmonary bypass. The flow was seeded with Al_2O_3 particles with a mean measured diameter of 48 μm. Water was used during the visualization tests using dye injection and the flow rate was estimated using Reynolds similitude between water and the water-glycerin solution.

2.3. Laser Doppler anemometry

A two-component fiber optic laser Doppler anemometer (DANTEC) was used to measure the axial and tangential velocity components. In this system a 4 W argon-ion laser was coupled to a fiber drive unit which allowed for a color separation of the primary beam. The resulting green (514.5 nm wavelength) and blue (488 nm wavelength) beams were used for the velocity measurements. A 160 mm focal length lens was coupled to the LDA probe to produce an ellipsoidal measurement volume with a maximum length, in air, of 0.658 mm and a diameter of 0,078 mm. The Doppler signal were processed with fast Fourier signal analyzer and a commercial software (Burstware) was used to acquire data and to control the signal analyzers and the photomultiplier. Approximately 3000 measurements were acquired for each spatial location. LDA measurements were done at four different planes labeled N, S, E and O. A coordinate system was adopted in order to perform the measurements. The system is oriented in such a way that x axis is directed radially, y axis axially and z axis is tangential to the filter. Z axis is horizontally directed and always parallel to the LDA probe surface. Figure 3 shows the measurement planes and their locations during the tests. The level was located 17 mm above the bottom surface from the support of the filtering element. Measurements were performed at fourteen points with a distance of 1,0 mm from each other. The first point was located 1,0 mm far from the wall. The tangential velocity (U) is positive in the negative sense of the z axis while the axial velocity (V) is positive following the y axis sense.

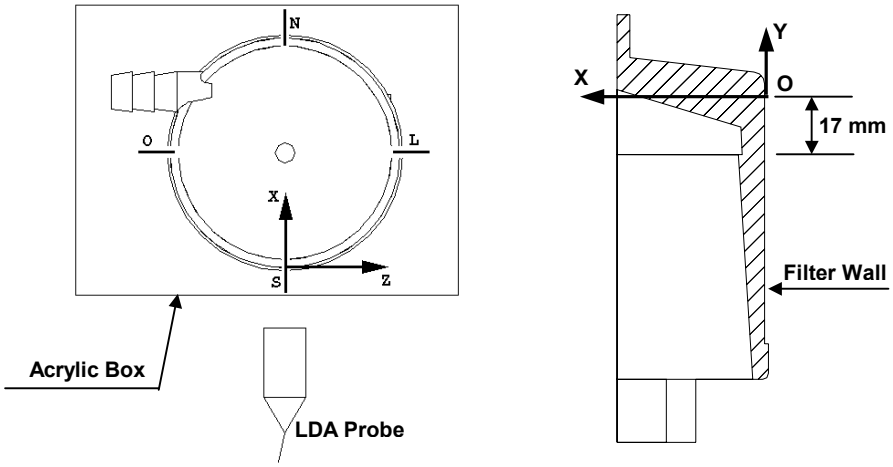

Figure 3 – Coordinate systems and measurements planes

The working fluid was a combination of 40%, in mass, of glycerin with 60% of water. This working fluid was chosen because it matches the blood transport properties. At 25°C, the blood analog fluid has a density of 1.09 g/cm^3 and absolute viscosity of 3.18 mPa.s. One problem associated with this working fluid when using a optical measurement technique is the refraction index. The measured refraction index of the solution was 1.383 which is lower than 1.49, the refractive index of the filter wall. This difference implies in a displacement of the LDA measurement volume due to the refraction of the laser beams. An equation that describes the position of the measurement volume inside the filter was developed using Snell´s law. Figure 4 shows the refraction of two laser beams crossing to materials with different refraction index. The beams should intercepted at O but they intercepted at O´ due to the difference between n_1 and n_2, the materials refraction indexes.

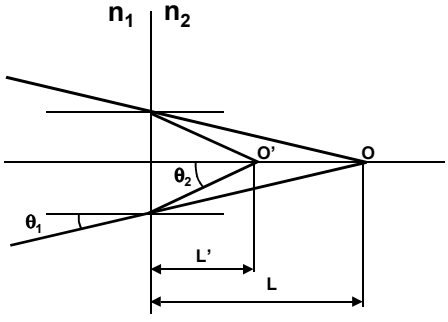

Figure 4 – Laser beams crossing two different materials

The equation that describes the correct position of the measurement volume is where θ_2 is evaluated using Snell´s law (Dybbs and Edwards, 1987).

$$\frac{L'}{L} = \frac{\operatorname{Tan}\theta_1}{\operatorname{Tan}\theta_2} \tag{2}$$

The instantaneous velocities ($\tilde{u}_n$ and $\tilde{v}_n$), measured by the LDA, can be separated into mean components (U and V) and fluctuating components (u_n e v_n). Mean velocities can be evaluated as

$$\overline{U} = \frac{\sum \tilde{u}_n \Delta t_n}{\sum \Delta t_n} \tag{3}$$

and

$$\overline{V} = \frac{\sum \tilde{v}_n \Delta t_n}{\sum \Delta t_n}, \tag{4}$$

where N is the number of collected samples. The fluctuating components are estimated using equations (5) and (6).

$$\overline{u^2} = \frac{\sum \left(\tilde{u}_n - \overline{U}\right)^2 \Delta t_n}{\sum \Delta t_n} \tag{5}$$

and

$$\overline{v^2} = \frac{\sum \left(\tilde{v}_n - \overline{V}\right)^2 \Delta t_n}{\sum \Delta t_n}. \tag{6}$$

The gate-time averaging technique was adopted in order to remove the “velocity bias” which, would lead to the overestimation of the velocity. Techniques for determining Reynolds stresses in stationary flows from LDA measurements are well established (Baldwin et all, 1993). Reynolds normal stresses ($\overline{\rho uu}$ e $\overline{\rho vv}$) and shear stress ($\overline{\rho uv}$) are determined by the following equations.

$$\overline{\rho uu} = \frac{1}{N}\sum \rho u_n^2, \tag{7}$$

$$\overline{\rho vv} = \frac{1}{N}\sum \rho v_n^2, \tag{8}$$

and

$$\overline{\rho uv} = \frac{1}{N}\sum_{1}^{N} \rho u_n v_n. \tag{9}$$

Normal and shear stresses were used to evaluate principal stresses. Principal stresses are estimated using the equation proposed by Higdon et all (1985)

$$\overline{\sigma}_{max,min} = \frac{\overline{\rho uu} + \overline{\rho vv}}{2} \pm \sqrt{\left(\frac{\overline{\rho uu} - \overline{\rho vv}}{2}\right)^2 + \overline{\rho uv}^2}, \tag{10}$$

and the maximum shear stress can then be obtained from the principal stresses as

$$\tau_{max} = \frac{1}{2}\left(\sigma_{max} - \sigma_{min}\right) \tag{11}$$

The magnitude of shear stresses acting on red blood cells and their exposure times to that shear fields are two parameters that have to be considered in the study of hemolysis induced by the flow. In the present work the exposure time was estimated considering the time necessary to the seeding particles to cross the LDA measurement volume. The

LDA measurement volume is an ellipsoid which was placed in the flow in such a way that the seeding particles cross it along his shortest axis. Exposure time is the result of the quotient between the axis length and the velocity vector modulus. The percentage of hemoglobin released by red blood cells was evaluated using the equation proposed by Wurzinger et al. (1985)

$$\%Hb = 3{,}62x10^{-5}\ t^{0.79}\ \tau_{max}{}^{2.4} \tag{12}$$

where t is the exposure time, in seconds, and τ_{max} is the maximum shear stress, in N/m^2. The turbulent kinetic energy was evaluated using the following equation.

$$ECT = \frac{\overline{u^2} + \overline{v^2}}{2} \tag{13}$$

2.4. Flow visualization

Flow visualization was done using the same test bench described before. Dye was injected, using a needle, through the inlet connector and eight orifices made at the upper part of the filter. At each orifice the dye was injected at three different levels. Figure 5 shows the injection points and levels. It must be pointed out that the nomenclature used to label the measurement planes was adopted to the injection points planes. Visualization was performed using a WEB camera placed normal to the filter surface in the region where the needle was placed.

Figure 5 – Injection points and levels

Water, at 25°C, was used as working fluid and Reynolds similitude was used to evaluate the flow rate. The similitude asserts that the flow pattern observed using water is the same that using the solution of water and glycerin.The characteristic length used in the Reynolds number evaluation was the diameter of the inlet connector.

$$\frac{\rho_{water} V_{water} D_{filter}}{\mu_{water}} = \frac{\rho_{sol.40\%} V_{sol.40\%} D_{filter}}{\mu_{sol.40\%}}. \tag{14}$$

Water flow rate can be expressed in terms of water-glycerin flow rate and kinematics viscosity as

$$Q_{water} = \frac{\nu_{water}}{\nu_{sol.40\%}} Q_{sol.40\%} = \frac{0{,}857}{2{,}898} 4{,}5 = 1{,}33\ (\text{l/min}) \tag{15}$$

3. Results and Discussion

3.1. Flow visualization

Figure 6 shows the flow visualization, at the upper part of the filter, at different instants of time. The left image shows a dye jet flowing through the inlet connector and achieving the opposite wall. The jet is deflected and tends to flow in direction of the E plane, in a clockwise sense and finally achieves the inlet connector. There is a white spot near the central region of the filter. This spot shows a recirculating flow which difficult the convective mass transport, thus dye dispersion but is high effective to retain air bubbles that can be removed through the bubble trap.

Figure 6 – Flow visualization at the upper part of the filter at three successive instants of time

Flow visualization at planes E, SE, S and SO is show at figure 7, respectively. At planes E, SE and S dye flows in a descending clockwise sense, showing that the velocity vector has at least two components, the tangential and axial. At plane SO the axial component vanishes and the dye has a horizontal trajectory. Figure 8 shows the flow visualization at planes O, NO, N and NE, respectively. At planes O, NO and N the flow has an ascending behavior, this mean that the axial velocity has a positive value and the blood is not collected by the outlet channel. The visualization at plane NE shows the incoming jet being divided because part of the dye flows in a clockwise sense, in direction of plane E while part of it flows in direction of the N plane. The flow coming from the NE plane interacts with the flow coming from the SO plane and both streams are affected by the low pressure area created by the incoming jet, thus an ascending flow happens in the region located between planes O and N.

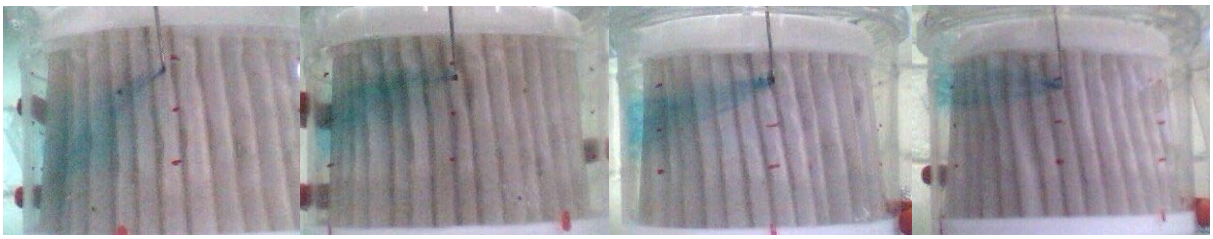

Figure 7 – Flow visualization at planes E, SE, S and SO, respectively

Figure 8 – Flow visualization at planes O, NO, N and NE, respectively

3.2. LDA measurements

Figure 9 shows the tangential velocity profiles for planes N and E. In plane N the velocity has a maximum absolute value of 1,4 m/s at 5 mm from the wall, which corresponds to the jet centerline. Velocity decrease as the distance to the jet centerline increases. Near the wall the velocity is 0 due to the no slip condition while at 10 mm from the wall the jet energy is almost dissipated by the recirculating zone at the filter center shown in figure 6. In the plane E the maximum value is 0,92 m/s and succeeds near the wall. At plane E the jet has achieved the wall and is deflected thus the velocity profile is distorted. The same behavior was observed in planes S and O, but with smaller maximum absolute values. In plane S the maximum value is 0.6 m/s while in plane O is 0,4 m/s.

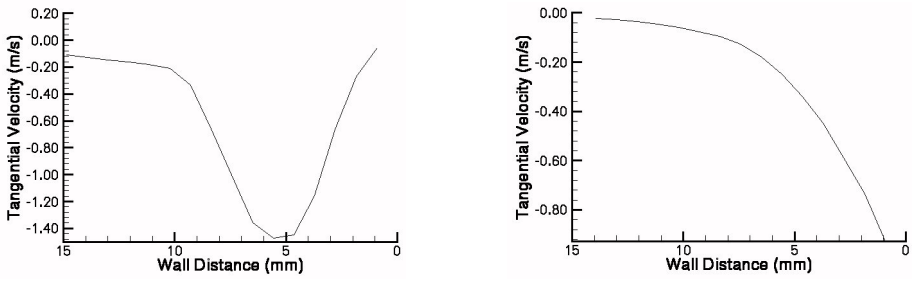

Figure 9 – Tangential velocities at the planes N and E, respectively.

Figure 10 shows the axial velocity profiles for planes N, E and W, respectively. Near the wall at plane N, the axial velocity is positive showing an ascending flow. At plane E, near the wall, the velocity is negative thus the flow has a descending behavior. In the planes W and S the component is very small thus the flow can be considered tangential. In all planes the axial velocity is null in the central region of the filter and oscillates in the area comprised the jet and the recirculation core.

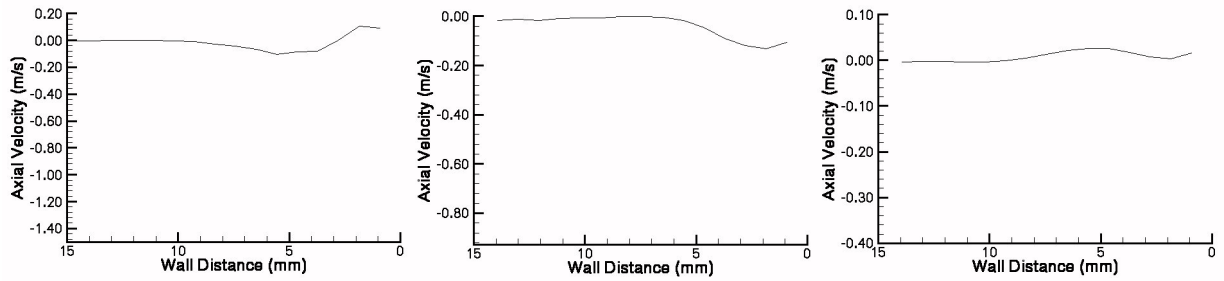

Figure 10 – Axial velocities at the planes N, E and W, respectively

In figure 11 the velocities root mean square at plane N is shown. Both profiles are similar and are the consequence of the jet interaction between the wall and the recirculation area at the filter center. These peaks, symmetrically disposed about the jet axis, correspond to the mixing layer between flows at low and high velocities (Hinze, 1987).

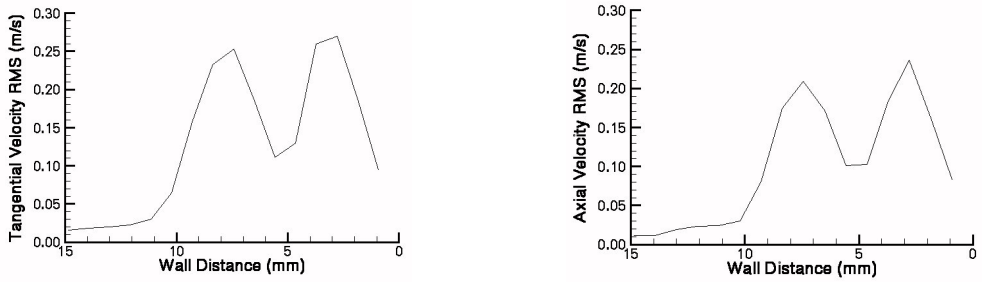

Figure 11 – Root mean square of the velocities at plane N

The maximum shear stress profile at plane N is shown in Figure 12. There is a spatial correspondence between maximum shear stress and mean velocity gradient, so that the "eddy viscosity" hypothesis (Hinze, 1987), which states a proportionality between Reynolds shear stress and mean velocity gradient, can be invoked (Grigioni et al., 2001). In the energy balance equation the energy production terms is proportional to the mean strain, therefore the regions of high velocity variations are naturally involved in turbulence generation.

The exposure time is also shown in figure 12. The profile indicates a maximum value near the central region of the filter where the velocity has a low value and the region between the jet and the wall where the flow field is influenced by the ascending flow described before.

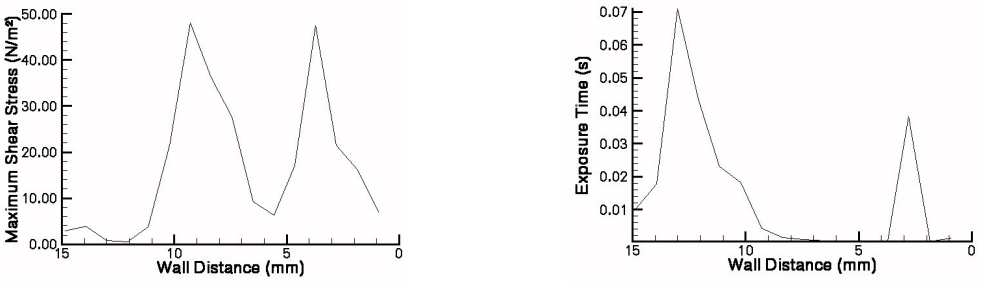

Figure 12 – Maxim shear stress and exposure time at plane N

The peaks of maximum shear stress and exposure time happen in the same region thus accordingly equation (1) proposed by Wurzinger (1985) the maximum percentage of released hemoglobin will happen in this area. Figure 13 shows the percentage of released hemoglobin profile at plane N. The profile has two peaks and the highest correspond to the point where the exposure time profile has a maximum. The maximum value of %Hb is 0,0060 and is very small compared to the value of 1,65 evaluated using the values of 800 N/m² and 1 ms proposed by Lu et al. (2001).

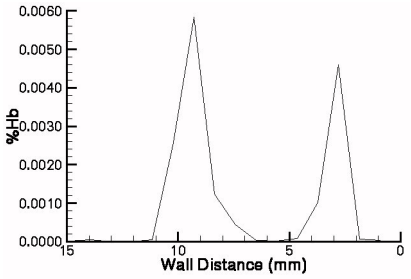

Figure 13 – Percentage of released hemoglobin profile at plane N.

4. Conclusions

This work reports the use of laser Doppler velocimetry to study the incoming flow in an arterial blood filter. A test bench was developed in order to allow the use of a LDA system and a working fluid with viscosity and density similar those of blood was used. Velocities profiles and their fluctuations were measured at four planes. Velocity fluctuations were used to evaluate turbulent shear stresses which were combined with the exposure time in order to evaluate the percentage of released hemoglobin. Results also indicate that the filter has a low tendency to damage red blood cells, considering the measured planes. The general flow structure was studied using the dye injection technique and the results are used to explain some LDA measurements results.

5. Acknowledgement

This work was financed by CNPq (Brazilian research council), grants n°200729/95-0 and n°300556/97-7. The contribution of S. Evangelisti to the LDA measurements and V. Ponzio to the construction of the experimental setup is gratefully acknowledged.

6. References

Baldwin, J.T., Deutsch, S., Petrie, H.L. & Tarbell, J.M., 1993, Determination of principal Reynolds stresses in pulsatile flows after elliptical filtering of discrete velocity measurements. Journal of Biomechanical Engineering, v.115, p.396-403.

Dybbs, A, and Edwards, R.V., 1987, Refractive index matching for difficult situations. Laser anemometry advances and applications.

Grigioni, M., Daniele, C., D'Avenio, G., and Barbaro, V., 2001, "The influence of the leaflet's curvature on the flow field in two bileaflet prosthetic heart valves", Journal of Biomechanics, vol. 34, pp. 613-621.

Grigioni, M., Daniele, C., Morbiducci, U., D'Avenio, G., Di Benedetto, G., Del Gaudio, C. and Barbaro, V., 2002,"Computational model of the fluid dynamics of a cannula inserted in avessel: inicidence of the presence of side holes in blood flow", Journal of Biomechanics, vol. 35, pp. 1599-1612.

Higdon, A.,Ohlsen, E.H., Stiles, W.B., Weese, J.A. and Riley, W.F., 1985, Mechanics of Materials. New York, NY : John Wiley & Sons.

Hinze, J.O., 1987, "Turbulence", McGraw-Hill, New York.

Lu, P.C., Lai, H.C. and Liu, J.S.,2001,"A reevaluation and discussion on the threshold limit for hemolysis in a turbulent shear flow", Journal of Biomechanics, vol. 34, pp. 1361-1364.

Paul, R., Schügner, F., Reul, H., Rau, G., (1999), "Recent findings on flow induced blood damage : critical shear stresses and exposure times obtained with a high shear Couette-system", Artificial Organs, v.23, n.7, p.680.

Rand, R.P., 1964, "Mechanical properties of red cell membrane. Part 2, Viscoelastic breakdown of the membrane", Biophysics, v.4, p.303-316.

Sallam, A.M., Hwang, N.H.C., 1984, "Human red blood cell hemolysis in a turbulent shear flow : contribution of Reynolds shear stresses", Biorheology, v.21, p.783-797.

Sutera, S.P., 1977, "Flow induced trauma to blood cells", Circulation research, v.41, n.1, p.2-8.

Sutera, S.P., Mehrjardi, M.H., 1975, "Deformation and fragmentation of human red blood cells in turbulent shear flow", Biophysical journal, v.15, p. 1-10.

Wurzinger, L.J., Opitz, R., Blasberg, P. e Schönbein, S., 1985, Platelet an coagulation parameters following millisecond exposure to laminar shear stress. Thrombosis and Haemostasis, v.54, n.2, p.381-386.

7. Copyright Notice